Photocatalytic Treatment of Wastewater Containing Simultaneous Organic and Inorganic Pollution: Competition and Operating Parameters Effects

Ahmed Amine Azzaz, Salah Jellali, Nasser Ben Harharah Hamed, Atef El Jery, Lotfi Khezami, Aymen Amine Assadi, Abdeltif Amrane

HAL Id: hal-03331070

https://hal.science/hal-03331070

Submitted on 1 Sep 2021

Photocatalytic Treatment of Wastewater Containing Simultaneous Organic and Inorganic Pollution: Competition and Operating Parameters Effects

Ahmed Amine Azzaz [1,2]**, Salah Jellali** [3]**, Nasser Ben Harharah Hamed** [4]**, Atef El Jery** [4]**, Lotfi Khezami** [5]**, Aymen Amine Assadi** [6] **and Abdeltif Amrane** [6,*]

1   Environnements DYnamiques et TErritoires de la Montagne, Université Savoie Mont-Blanc, EDYTEM, 5 Boulevard de la Mer Caspienne, 73370 Le Bourget-du-Lac, France; ahmed-amine.azzaz@univ-smb.fr
2   Water Research and Technologies Center, Wastewater Treatment Laboratory, University of Carthage, P.O. Box 273, Soliman 8020, Tunisia
3   Center for Environmental Studies and Research, PEIE Research Chair for the Development of Industrial Estates and Free Zones, Sultan Qaboos University, Al-Khoud 123, Oman; s.jellali@squ.edu.om
4   Department of Chemical Engineering, College of Engineering, King Khalid University, Abha 61411, Saudi Arabia; hhharharah@kku.edu.sa (N.B.H.H.); ajery@kku.edu.sa (A.E.J.)
5   Department of Chemistry, College of Sciences, Imam Mohammad Ibn Saud Islamic University, P.O. Box 5701, Riyadh 11432, Saudi Arabia; lkhezami@gmail.com
6   Ecole Nationale Supérieure de Chimie de Rennes, Université de Rennes, CNRS, ISCR-UMR 6226, 35000 Rennes, France; aymen.assadi@ensc-rennes.fr
*   Correspondence: abdeltif.amrane@univ-rennes1.fr; Tel.: +33-(0)-2-23-23-40-00

Abstract: In the present study, methylene blue (MB) removal from aqueous solutions via the photocatalytic process using TiO_2 as a catalyst in the presence of external ultra-violet light (UV) was investigated. The results of adsorption in the absence of UV radiation showed that adsorption reached an equilibrium state at 60 min. The experimental kinetic data were found to be well fitted by the pseudo-second-order model. Furthermore, the isotherm study suggested that dye uptake by TiO_2 is a chemisorption process with a maximum retention capacity of 34.0 mg/g. The photodegradation of MB was then assessed under various experimental conditions. The related data showed that dye mineralization decreased when dye concentrations were increased and was favored at high pH values and low salt concentrations. The simultaneous presence of organic and inorganic pollution (Zinc) was also evaluated. The effect of the molar ratio Zn^{2+}/MB^+ in the solution at different pH values and NaCl concentrations was also monitored. The corresponding experimental results showed that at low values of Zn^{2+} in the solution (30 mg/L), the kinetic of the MB removal became faster until reaching an optimum at Zn^{2+}/MB^+ concentrations of 60/60 mg/L; it then slowed down for higher concentrations. The solutions' carbon contents were measured during the degradation process and showed total mineralization after about 5 h for the optimal Zn^{2+}/MB^+ condition.

Keywords: combined pollution; methylene blue; heavy metal; adsorption; photocatalysis

1. Introduction

Nowadays, the integrated management of surface or underground water resources has become an absolute necessity to compensate for accelerating demographic growth; the intensification of human activities, particularly in the industrial and agricultural sectors; and the improvement of the life quality of several countries. In this context, the preservation of water quality, whether intended for human consumption, for irrigation or simply to be discharged into nature, towards rivers, oceans or the ground, has become a significant challenge for all those concerned with protection of the environment. The textile industry is considered one of the most polluting sectors due to the discharge of contaminated effluents containing various toxic chemicals [1]. These effluents, when disposed of in the receiving bodies without an adequate prior pretreatment, could cause the degradation of surface

and underground water quality, thus negatively affecting human and animal lifestyle and health [2].

Among the pollutants abundantly found in textile effluents, dyes contribute to the quasi-totality of their Total Organic Carbon (TOC) content [3]. Despite their great importance to the international economy and especially to the industrial sector, these organic molecules are widely known for their harmful effects on ecosystem stability and sustainability. The seriousness of these pollutants stems from the fact that certain dyes are considered carcinogenic, mutagenic, and teratogenic for humans and can induce catastrophic effects on the water environment (wadis, rivers, water tables, etc.). Their severity is accentuated by the fact that most of them are poorly biodegradable, making natural mitigation of this type of pollution challenging to achieve.

To face such problematic occurrences, the scientific community has become oriented towards the elimination of dyes from aqueous solutions by applying technologies such as adsorption [4], coagulation-flocculation [5], and phytoremediation [6]. Although some of these methods could lead to respectable dye-removal capabilities, they generate a considerable quantity of by-products and sludge that requires additional procedures to be treated. Thus, advanced oxidation processes (AOPs) have emerged as a compelling and promising method for dye-rich wastewater treatment. This technique is known for being flexible, highly efficient toward organic compounds, and leads to the generation of a minimum quantity of residuals compared with other processes [3,7–9]. By begetting strong oxidizing radicals such as $^\bullet OH$, AOPs trigger a succession of chemical reactions in the solution, leading the electronic links of the dye molecule to break into smaller components, called oxidation byproducts, until total mineralization of the hazardous pollutant, to yield finally carbon dioxide [10–16]. Various AOPs were employed in this purpose, such as Fenton [17], Photo-Fenton [5], ozonation [7], and sonolysis [8]. The heterogeneous photocatalysis method has largely drawn scientific attention [18]. It is mainly based on the use of UV-irradiated semi-conductors creating electron-hole pairs and entering into a reaction with OH^- before being adsorbed onto the surface of the semiconductor, leading to the creation of oxidizing $^\bullet OH$ and $O_2^{\bullet-}$ radicals [16].

However, most of these studies have focused on removing pure or mixed organic compounds from synthetic solutions without considering the complex composition of real wastewaters, especially their simultaneous richness in organic and inorganic pollutants such as metals [19]. A photocatalytic process for wastewater treatment containing combined pollution was avoided because organic and inorganic compounds have different behavior in the presence of UV radiation, not to mention their high sensibility to the governing pH of the solution and the possible interactions that could occur between the two different types of compounds and the photocatalyst.

The main goals of this study were as follows: (i) the determination of the principally involved mechanisms during MB adsorption onto the photocatalyst before UV-irradiation, (ii) investigations into MB removal from aqueous solutions during UV-irradiation under various experimental conditions, and (iii) assessment of the impact of the presence of a heavy metal on MB removal efficiencies.

2. Results and Discussion

2.1. Water Treatment Studies in the Case of Single-Type Pollution

2.1.1. Kinetic and Isotherm Adsorption of MB onto TiO$_2$ Prior UV-Irradiation

The photodegradation of dye from aqueous solutions using UV-irradiation in the presence of a photocatalyst mainly functions as the studied pollutant's adsorption capacity on the surface of the semiconductor. To understand the mechanisms involved in this process, a preliminary study of dye uptake by titania was made in the absence of UV-irradiations, including kinetic and isotherm experiments at different times and initial MB concentrations.

The adsorption of MB onto TiO$_2$ powder was investigated to reach a concrete idea of the photocatalyst's adsorptive capacity before the irradiation phase. A kinetic study was

performed for contact times varying between 1 and 180 min at an initial MB concentration of 60 mg/L. As could be remarked in Figure 1, MB retention onto TiO_2 is a time-depending process, characterized by a rapid increase in the adsorbed dye quantity (qt; mg/g), especially at early reaction times, i.e., up to 20 min of contact time, where it reached 80% of the adsorbed amount. At extended adsorption times, the uptake tendency seemed to slightly increase but with a much slower trend until it reached an equilibrium at 90 min. It has been reported that the early hard slope is related to the quick adsorption rate of MB molecules on the surface by occupying free functional groups, followed by a slower intra-particle diffusion mechanism [3,20]. Similar findings were reported by Wang et al. [14,21], when studying the removal of MB using Polyaniline/TiO_2 hydrate particles.
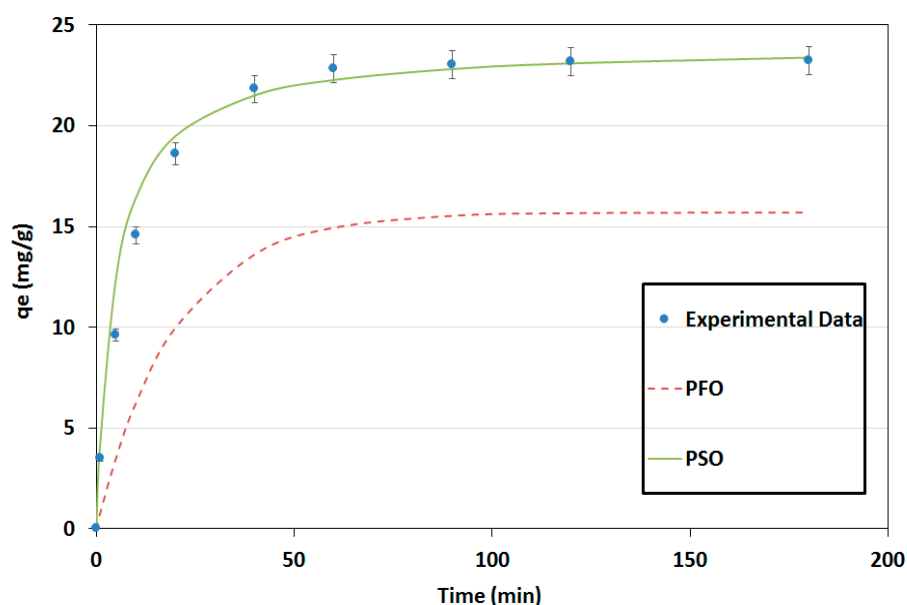

Figure 1. MB kinetic adsorption onto TiO_2 and their fitting by pseudo-first-order and pseudo-second-order kinetic models (C_0 = 60 mg/L; pH neutral; D_{TiO_2} = 1 g/L; temperature = 20 ± 2 °C).

To reach an appropriate understanding of the possible retention mechanisms, pseudo-first and second-order models were applied, expressions of which are widely found in the literature [10]. According to the results gathered in Table 1, both models presented high correlation coefficients, which suggests their suitability for the experimental data. Nevertheless, the theoretical adsorbed quantity related to the pseudo-first-order model ($q_{e,I}$; mg/g) does not fit the experimental result, which proposes that MB adsorption onto titania cannot be considered a pseudo-first-order mechanism. The different outcome was remarked for the Lagergren pseudo-second-order model, where the $q_{e, II}$ (mg/g) value was very close to the experimental data. This observation was further confirmed by the calculated error where PSO's APE values were 5 times less significant than the one found for the PFO model. Accordingly, the adsorption of MB could be attributed to a chemical reaction between the molecule and the TiO_2 surface functional groups [11–14]. It is probable that the adsorption of MB onto titania at pH values slightly superior to the pH_{zpc} (6.7) is due mainly to the hydroxyl and oxygen ligands present on its surface, offering functional fixing sites to the dye molecule, in addition to the retention caused by the important specific surface of the semiconductor [16,18]. Similar observations were cited by Jafari et al. [22] when studying the adsorption of a cationic dye, i.e., methyl violet (MV), onto TiO_2 nanoparticles. The authors suggest that the retention of the MV molecule was not physically driven as the kinetic adsorption rate did not increase with increasing particle size, limiting the intraparticle diffusion mechanism. However, the study emphasized the possible involvement of two types of surface functional groups, namely Ti–OH and

Ti–O–Ti, where these oxygenic sites are favorable for retaining a cationic dye either via proton liberation or electrostatic binding [23].

Table 1. Kinetic parameters for MB adsorption onto TiO_2.

		Pseudo-First-Order				Pseudo-Second-Order			
	$q_{e,exp}$ (mg/g)	K_1 (min^{-1})	$q_{e,I}$ (mg/g)	R^2	APE (%)	K_2 (g/mg.min)	$q_{e,II}$ (mg/g)	R^2	APE (%)
TiO_2	23.04	0.05	15.678	0.9748	46.159	0.009	23.98	0.9988	8.492

The initial dye concentration effect on adsorption efficiency was also investigated, and the results were depicted in Figure 2 and Table 2. The MB uptake increased significantly with increasing initial dye concentration. The increase of the MB aqueous concentration from 30 to 180 mg/L permitted the TiO_2 to increase its retention capacity from 13.43 to 29.63 mg/g, respectively (Figure 2). This result is related to two factors: (i) the presence of a higher amount of dye molecules in the solution increases the probability of their fixation on the functional groups of the adsorbent, and (ii) the increase of dye concentrations is proportional to the diffusion gradient between aqueous and solid phases [24,25]. Langmuir and Freundlich's models were used to predict the fixation mechanism of MB molecules on the titania surface [10].
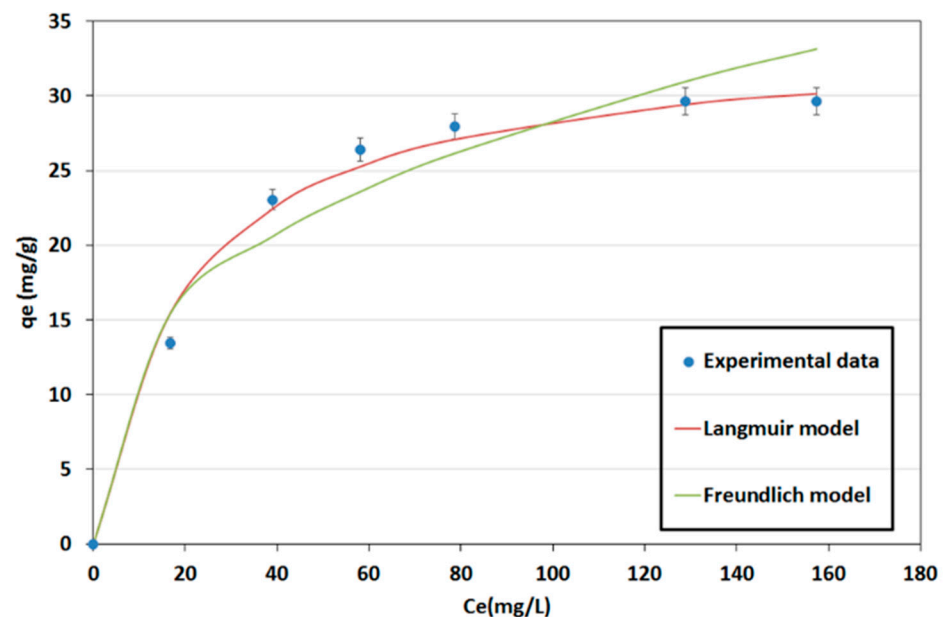

Figure 2. MB adsorption onto TiO_2 at equilibrium and their fitting by Langmuir and Freundlich, isotherm models ($C_{0, MB}$ = 30–180 mg/L, contact time = 90 min, pH neutral, D_{TiO_2} = 1 g/L; temperature = 20 ± 2 °C).

Table 2. Isotherm parameters for MB adsorption onto TiO_2.

		Langmuir				Freundlich		
	q_L (mg/g)	K_L	R_L	R^2		K_F	n	R^2
TiO_2	34.013	0.049	8.532×10^{-4}	0.9956		5.891	2.928	0.8626

The calculated APE was about 4.6% for the Langmuir model, suggesting that adsorption through a monolayer fixation process is probable. The maximal uptake capacity "q_{max}" of MB onto TiO_2 was about 34.0 mg/g. Moreover, the Langmuir coefficient value was lower than 1, which indicates the efficiency of MB adsorption by titania. On the other hand, Fre-

undlich's model suggests that adsorption occurs with a non-uniform distribution of heat in the presence of a heterogeneous surface. The calculated APE for this model was about 9.8%, two times higher than the one found for the Langmuir model. The Freundlich exponent coefficient "n" was 2.9, belonging to the range of 1–10, which indicates that the adsorption of dye on the semi-conductor was favorable [26]. Thus, the chosen model has lower AEP and a higher correlation coefficient (0.996 and 0.863, for Langmuir and Freundlich models, respectively). The choice was made in favor of the Langmuir model, presenting a good fit to experimental data (Figure 2). Therefore, the retention of MB could be assigned to a thermodynamically spontaneous, homogeneous, and monolayer distribution onto TiO_2 particles [19].

To investigate the TiO_2 efficiency for the adsorption of MB compared with other photo-catalysts, a comparison, based on the Langmuir maximal retention capacity "q_{max} (mg/g)", was accordingly achieved (Table 3). It could be remarked that the current photocatalyst presents an almost similar retention capacity for Methylene Blue as bentonite-titanium dioxide composites [27] or rectorite-based magnetic zinc oxide [28]. However, it has a lower adsorption capacity than graphene oxide particles [29] or bentonite-ZnO-CuO composite [30]. Therefore, TiO_2 (Anatase) nanoparticles could be considered as an exciting adsorbent for MB molecules. This capacity could be further enhanced if the semi-conductor is modified chemically and/or physically to improve their surface properties for the adsorption of dyes, as well as their photocatalytic functionalities.

Table 3. Comparison of MB adsorption onto TiO_2 nanoparticles and other photocatalysts.

Material	C_0 (mg/L)	Adsorption Capacity (mg/L)	Refs.
Bentonite-titanium dioxide composites	200	48.45	[27]
Graphene oxide-based material	125	120.48	[29]
Rectorite-based magnetic zinc oxide	50	35.10	[28]
Encapsulated biochar-supported nanoscaled zinc oxide	300	17.01	[31]
Bentonite-ZnO-CuO composite	100	166.11	[30]
ZnO/montmorillonite	10	6.56	[32]
TiO_2 nanoparticles	180	29.63	Present study

2.1.2. Photocatalytic Degradation of MB at Different Experimental Conditions

The photocatalytic elimination of MB under UV-irradiation was performed in batch mode to investigate the degradation performance of TiO_2 in terms of organic dye removal under different experimental conditions. Before launching the desired manipulation by starting the UV lamp, the solution was kept in a dark condition until dye adsorption onto TiO_2 reached equilibrium.

Influence of the Photocatalyst Dose

Since photodegradation is a process that occurs on the catalyst surface, the increase in the TiO_2 dose in the solution was expected to increase the degradation rate due to the rising number of adsorption sites on its surface [33–38]. The catalyst doses' effect on the dye photodegradation process is presented in Figure 3. It could be remarked that the increase in the titania dose gradually increased the degradation rate of MB by reaching an optimum at 1 g/L, presenting a total bleaching dye capacity at 55 min for an initial concentration of 60 mg/L. The photodegradation of MB could be considered as a PFO reaction. To quantify the MB degradation efficiency using TiO_2, the PFO model was determined by plotting the curve: $ln\left(\frac{C}{C_0}\right) Vs. - kt$, where C and C_0 are the initial dye concentration and the dye concentration (mg/L) for a given time t (min), respectively, and k is the apparent rate constant (min^{-1}). The degradation rate constants were found to be 0.0584, 0.0801 and

0.0533 for TiO$_2$ using doses of 0.5, 1, and 1.5 g/L, respectively. The degradation rate increased up to 7.1% for an increase in the catalyst dose from 0.5 to 1 g/L. Once this loading quantity was surpassed, the degradation process decreased by about 33.5%, allowing total discoloration after a contact time of 90 min. This behavior is mainly due to the possible screen effect in the batch reactor caused by TiO$_2$, preventing UV radiation from penetrating through the solution and activating the functional sites. Comparable results were recorded by Moussa et al. [16] when studying the removal of orange II dye using ZnO rods/reduced graphene oxide composites. Likewise, Sun et al. [18], when investigating the elimination of methylene blue by UV irradiation, employed the photocatalytic ability of reduced-graphene-oxide-modified TiO$_2$, ZnO and Ta$_2$O$_5$ semi-conductors. For the rest of the experiments, a photocatalyst dose of 1 g/L was used.
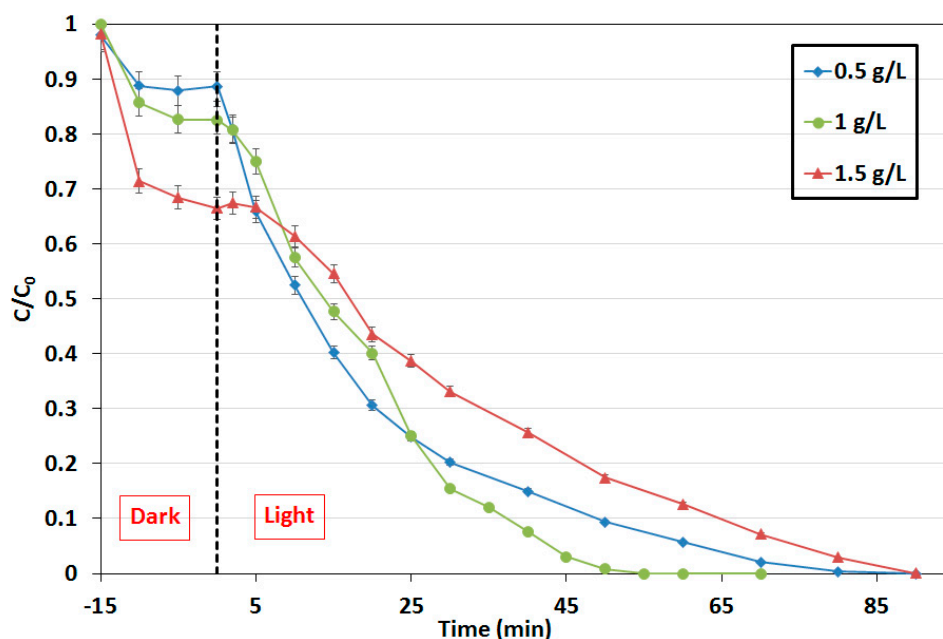

Figure 3. Influence of the TiO$_2$ photocatalyst mass for the degradation of MB in aqueous solution (C$_0$ = 60 mg/L; pH neutral; temperature = 20 ± 2 °C).

Effect of Dye Concentration

The effect of the initial MB solution concentration on its discoloration under UV radiation was investigated, and the corresponding results are illustrated in Figure 4. It appears that the photodegradation process depends intimately on the initial pollutant concentration.

Discoloration efficiency decreased with increasing MB concentration. Total bleaching of the MB was reached at 40 and 160 min of irradiation for initial dye concentrations of 30 and 90 mg/L, respectively. The calculated PFO model for each concentration and their related plots (Figure 5) delivers an abatement in the apparent rate constant by increasing the initial dye concentration (K (min^{-1}) = 0.1713, 0.0801, 0.0359 and 0.0051 for initial MB concentrations of 30, 60, 90, and 120 mg/L, respectively).

These results suggest that the MB concentration in solution and the amount of dye adsorbed onto the TiO$_2$ surface were proportional, owing to the growth of the intra-particular diffusion rates. The increase in adsorbed MB decreased the amount of incident UV irradiation penetrating through the TiO$_2$ particles to activate the reactive oxygen species and generate smaller amounts of •OH radicals. Similar findings were found in other studies [9,19,38].

Effect of pH

Methylene blue mineralization throughout UV-irradiation was observed for different initial pH and initial dye concentrations. Corresponding results were displayed in Figure 6a.
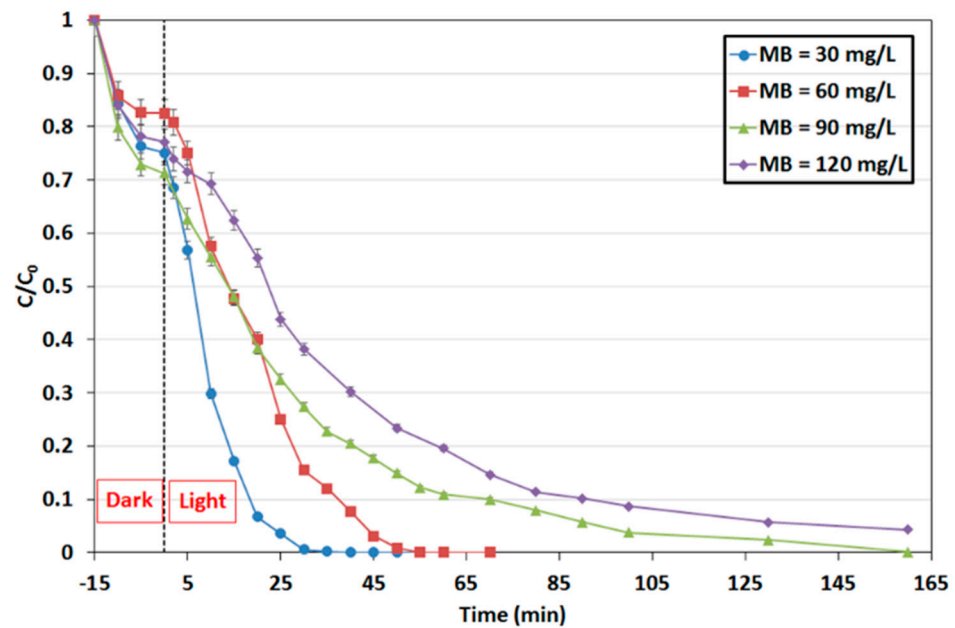
Figure 4. Influence of the MB concentration of the catalytic activity of the TiO$_2$ photocatalyst (pH neutral; D$_{TiO_2}$ = 1 g/L; temperature = 20 ± 2 °C).

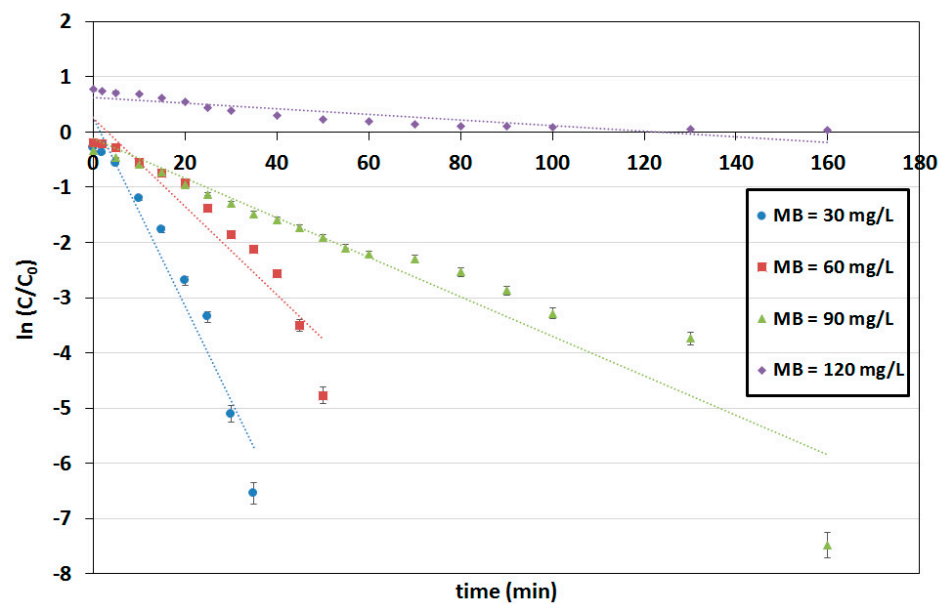**Figure 5.** Pseudo-first-order model for the MB concentration effect on photocatalytic activity, fitted to their linear plots (pH neutral; D$_{TiO_2}$ = 1 g/L; temperature = 20 ± 2 °C).

As it can be seen in Figure 6a, the photodegradation rate was greater in the basic solutions and decreased as the initial pH decreased. The MB bulk concentration diminished with the rise in pH after 15 min of irradiation, i.e., 36.7 and 13.8 mg/L for pH 4 and 8, respectively. Additionally, the photodegradation data were well described by the pseudo-second-order kinetics model, regardless of pH values. The reaction rate constants increased as the surrounding solution alkalinity increased, i.e., 0.0183, 0.0271, 0.0842, and 0.1025 min^{-1} for pH values 4, 5, 6, and 8, respectively.

These findings are mainly associated with the probable repulsion-attraction phenomenon occurring between the positively charged dye molecules on the one hand and the

TiO$_2$ surface with dominating charges in the solution on the other. In fact, for pH greater than pH$_{zpc}$ values, the dominating equation could be expressed as follows [19]:

$$Ti - OH + H^+ \leftrightarrow TiOH_2^+ \tag{1}$$

For pH < pH$_{zpc}$, the equation could be written as:

$$Ti - OH + OH^- \leftrightarrow TiO^- + H_2O \tag{2}$$
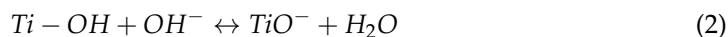
Therefore, for MB, known as a cationic dye, the anions excess (OH^-) due to the high pH value switch the dominating charge on the surface of TiO$_2$ above pH$_{zpc}$, allowing dye fixation and consequently enhancing the degradation process. It is also important to point out that the solution's final pH tends to decrease for high pH values and increase for initial acid solutions (see Figure 6b). The photodegradation equilibrium reaction of methylene blue may be written as follows [4]:
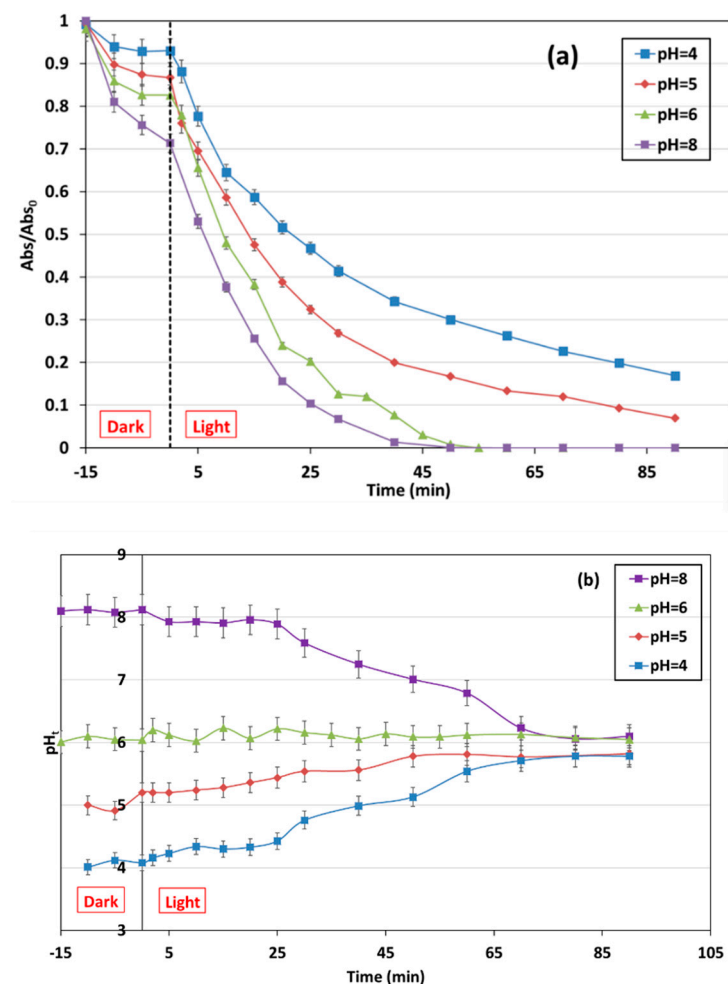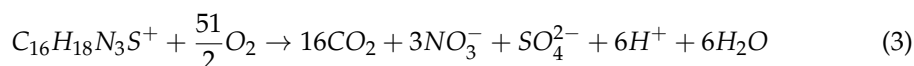
$$C_{16}H_{18}N_3S^+ + \frac{51}{2}O_2 \rightarrow 16CO_2 + 3NO_3^- + SO_4^{2-} + 6H^+ + 6H_2O \tag{3}$$

Figure 6. (**a**) Influence of the aqueous solution pH on the degradation of MB (C$_0$ = 60 mg/L; D$_{TiO_2}$ = 1 g/L; temperature = 20 ± 2 °C); (**b**) variation of pH in solution through the MB photodegradation process (C$_0$ = 60 mg/L; D$_{TiO_2}$ = 1 g/L; temperature = 20 ± 2 °C).

According to the Equations (1) and (2), one can suppose that, in presence of titania, the UV-irradiation process is tightly related to the pH$_{zpc}$ of the semi-conductor (pH$_{zpc}$ = 6.7), the dissociation equilibrium of water, and the ionization status of the organic

material. The degradation of MB generates more protons, which increases the overall pH. Furthermore, the effect of pH was more significant after the first 25 min of irradiation, due to the consumption of protons according to the Equation (1) and to the formation of $NO_3{}^-$ ions resulting from the photodegradation process.

Effect of Ion Competition

To simulate a real industrial effluent containing regularly additional ions, the effect of adding NaCl with different concentrations to the methylene blue solution was studied, and the obtained results are exhibited in Figure 7. It could be easily seen that salt concentration altered the adsorption of MB dye onto the TiO_2 surface. The MB concentration in the solution at equilibrium and before UV-irradiation varied from 44.4 mg/g to 60.1 mg/g for NaCl concentrations of 0 and 0.1 M, respectively. At low NaCl concentrations, the degradation rate was found to be slightly faster than the one recorded in the default experiment, i.e., [MB] = 60 mg/L, pH = 6, [NaCl] = 0 M. Several studies showed that sodium chloride positively affects the photodegradation of organic pollutants due to the generation of active chlorine, represented by hypochlorous acid and hypochlorite ions proportionally to the acidity of the solution [24]. According to Figure 7, an optimum point seems to be reached at a salt concentration of 0.001 M, inversely to the degradation rate of the dye occurring at high NaCl concentrations. It has been reported in the literature that high concentrations of ions present in aqueous solutions could compete with dye molecules for oxidative species, thus preventing the generation of •OH from reducing the degradation of MB. The pseudo-first-order reaction rate constant was calculated for the MB degradation in the case of the tested NaCl concentrations and found to be equal to 0.0929, 0.0796, and 0.0551 min^{-1} for 0.001, 0.01, and 0.1 M of NaCl, respectively. The results prove that the MB photodegradation reaction tends to be reduced by increasing the salt concentration.
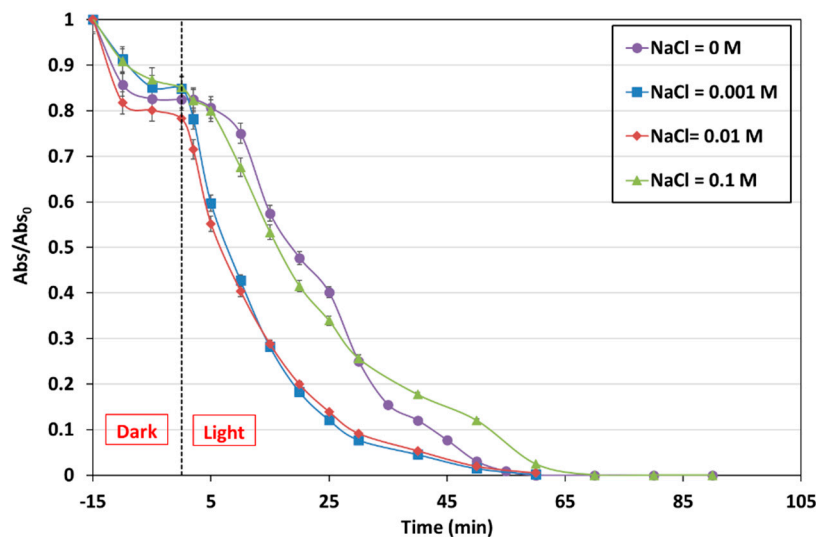

Figure 7. Influence of the aqueous solution salinity in the presence of NaCl ions on the degradation of MB (C_0 = 60 mg/L; pH neutral, D_{TiO_2} = 1 g/L; temperature = 20 ± 2 °C).

2.2. Water Treatment in the Case of Combined Pollution: Effect of Initial Dye and Heavy Metal Concentrations

In this section, the photodegradation of methylene blue in the presence of zinc was investigated. The effect of the variation of the initial dye and metal concentrations, pH, and the presence of salt were documented. In order to get a better understanding of the possible interactions that might occur during the photodegradation of the dye in presence of a heavy metal, a mimic industrial wastewater with different MB and Zn concentrations was prepared. The manipulations followed the experimental matrix, displayed in Table 4. The kinetic variations of MB concentration during photocatalysis are gathered in Figure 8a.

Table 4. Matrix of experiments to determine the UV-photocatalysis of methylene blue in the presence of zinc (mg/L) (pH neutral, $T° = 20 \pm 2$ °C, $D_{TiO_2} = 1$ g/L).

$\dfrac{[Zn^{2+}]}{[MB]}$	30	60	90	120
30	1	2	3	4
60	1/2	1	3/2	2
90	1/3	2/3	1	3/2
120	1/4	1/2	2/3	1
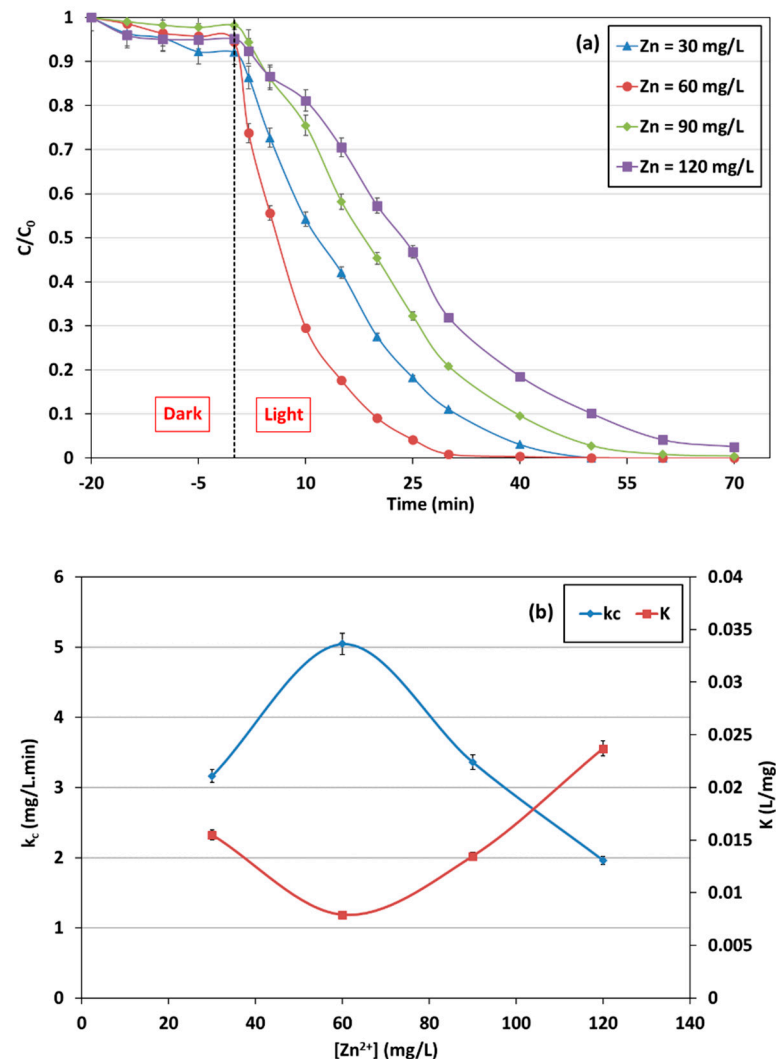
Figure 8. (**a**) Effects of zinc on the MB degradation photocatalytic efficiency of the used TiO$_2$ under UV-irradiation (C$_{0, MB}$ = 60 mg/L, pH neutral, D$_{TiO_2}$ = 1 g/L; temperature = 20 $\pm$ 2 °C); (**b**) Langmuir-Hinshelwood parameters related to the degradation of MB in aqueous solution in the presence of zinc (C$_{0, MB}$ = 30–120 mg/L, C$_{0, Zn^{2+}}$ = 30–120, pH neutral, D$_{TiO_2}$ = 1 g/L; temperature = 20 $\pm$ 2 °C).

The plot shows that the MB elimination changed dramatically by adding various zinc ions in the presence of UV-radiations. In fact, for low concentrations (30–60 mg/L), the degradation of MB seems to be enhanced. For instance, the concentration recorded at 40 min of irradiation in the absence of zinc and at a heavy metal concentration in an aqueous solution of 60 mg/L were 4.1 mg/L and 3.6 mg/L, respectively. However, by increasing the heavy metal concentration (90–120 mg/L), the degradation kinetic decreased remarkably, and the MB concentration raised to 19.9 mg/L for the same irradiation time and for a Zn^{2+} concentration of 120 mg/L.

To understand the kinetic and adsorption processes of MB degradation in the presence of a heavy metal, the Langmuir-Hinshelwood model was considered, and the corresponding results are gathered in Figure 8a,b.

To determine the parameters governing the photocatalytic process, the Langmuir-Hinshelwood model was used according to the following equation:

$$V_i = -\frac{dC_i}{dt} = \frac{k_c K C_i}{1 + K C_i} \tag{4}$$

where V_i (mg/L.min) is the initial photocatalytic degradation rate, C_i is the initial MB concentration (mg/L), k_c is the kinetic constant (mg/L.min) and K is the adsorption constant (L/mg).

The previous expression could be linearized and written as follows:

$$\frac{1}{V_i} = \frac{1}{k_c K} \times \frac{1}{C_i} + \frac{1}{k_c} \tag{5}$$

The curve $1/V_i$ versus $1/C_i$ was plotted in order to determine the k_c and K values. The kinetical constant and the adsorption constant were found to be 1.654 mg/L min and 0.066 L/mg, respectively ([MB] = 60 mg/L and [Zn^{2+}] = 60 mg/L).

According to Figure 8.b, the kinetic constants (k_c) calculated for all the experiments, cited in Table 4, show a distinguished pattern, symbolized by an increase for zinc concentrations varying from 30–60 mg/L, then a decrease for a zinc concentration going from 60 to 120 mg/L. On the other hand, the inverse variation was recorded for the adsorption constant K, decreasing at low concentrations of zinc (Figure 8b). For all the experiments performed in batch mode, the zinc concentration remained unchanged. This is mainly due to the repulsion process that occurs between the positively charged metal ions and the Ti^{4+}. This variation was noticed after calculating the reaction rate constant, especially at low and high metallic constants (K (min^{-1}) = 0.1253, 0.0622, 0.0563 and 0.0536 for [Zn^{2+}]/[MB] = 30/30, 30/60, 30/90 and 30/120; K (min^{-1}) = 0.0729, 0.0611, 0.0526 and 0.0385, for [Zn^{2+}]/[MB] = 120/30, 120/60, 120/90 and 120/120, respectively)

Zinc is known as a transition metal. Adding this metal to a semi-conductor in the solution lowers the summation and then the recombination of photogenerated electrons and holes. Thus, it contributes to the formation of more free radicals and improves the TiO_2 response already existing in the media, which leads to more UV-radiation adsorption and the enhancement of dye degradation [39]. Referring to Azzaz et al. [19], the possible reactions that might be occurring in presence of zinc could be presented in the following Figure 9:
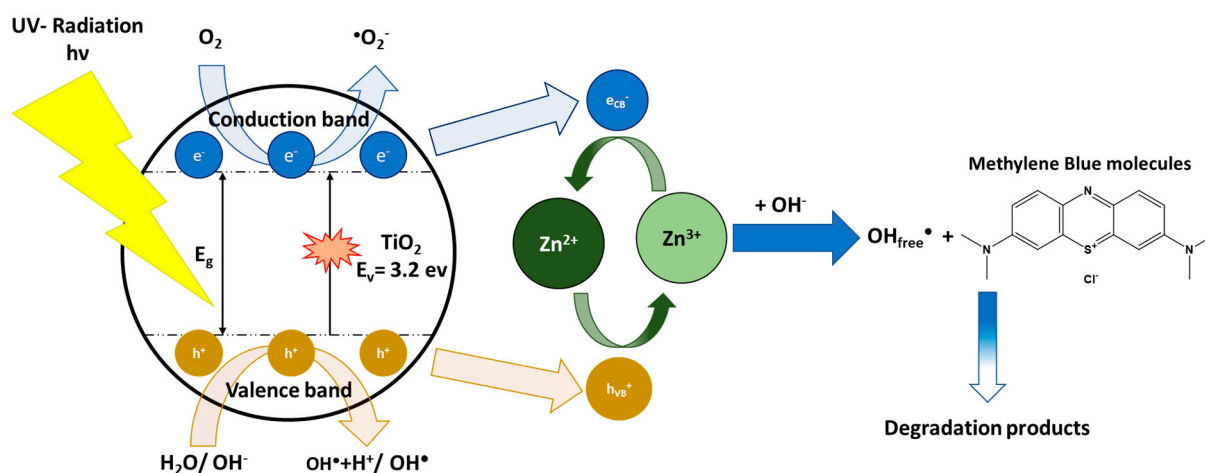

Figure 9. Schematic presentation of the methylene blue degradation mechanism under photocatalytic activation of TiO_2 in the presence of zinc ions in aqueous solution.

Therefore, zinc ions enter into a reaction with free electrons, then with dioxygen or hydroxide to form free radicals, and afterwards regain their initial electronic form. This incorporation at relatively low initial concentrations enhances the degradation of MB and its mineralization.

According to Figure 10, the TOC variation is characterized by decreasing organic content in the solution with an increase in irradiation time. It also depends on the initial concentrations of dye and zinc ions. By following the variation of initial organic pollution, the degradation percentage for 50 min of irradiation was equal to 52.1% and 40.2% for the initial $[Zn^{2+}]/[MB]$ concentrations of 30/30 and 30/60, respectively. The same trend was found when the initial zinc concentration was increased. Indeed, the degradation percentage varied from 52.1% to 36.6% after 50 min of irradiation for initial $[Zn^{2+}]/[MB]$ concentrations of 120/30 and 120/60, respectively.
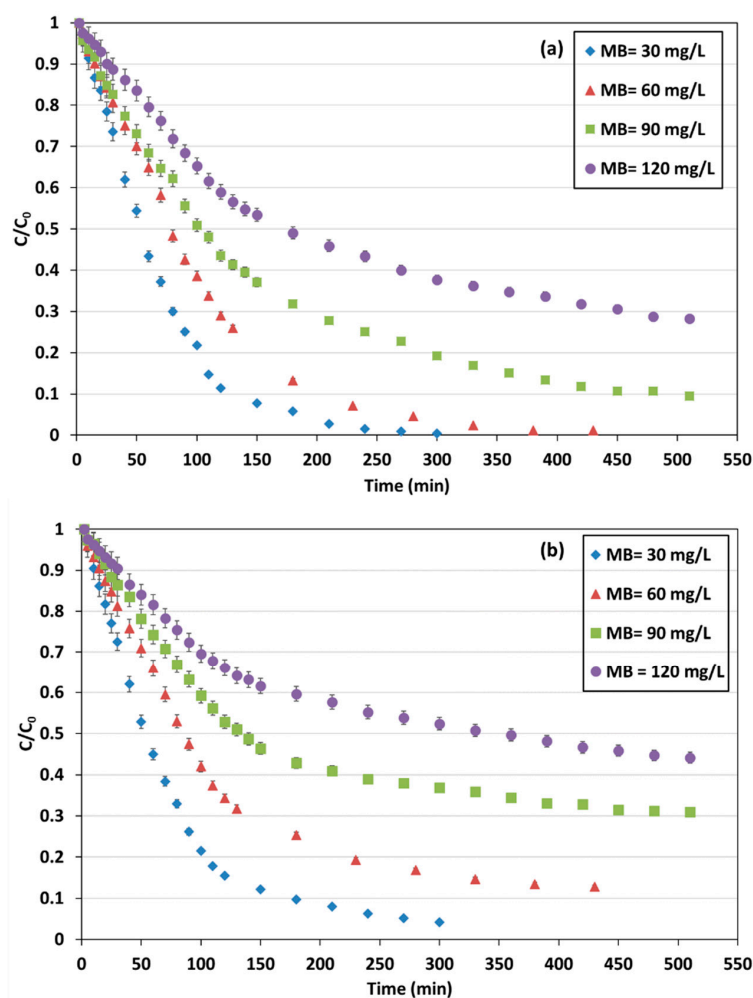

Figure 10. Aqueous solution COT variation for MB degradation under UV-irradiation for (**a**) low (30 mg/L) and (**b**) high (120 mg/L) zinc concentrations ($C_{0, MB}$ = 30–120 mg/L, pH neutral, D_{TiO_2} = 1 g/L; temperature = 20 ± 2 °C).

At the beginning of the reaction for neutral pH value, the solution is inclined to be slightly acid according to Equation (2). At pH values superior to TiO_2 pH_{zpc}, the semi-conductor triggers a reaction with hydroxide to form TiO^-, thus providing a more adsorbent function to the MB molecules. The increase in the adsorption of dye on the surface of the catalyst shifted to the conduction band, inducing the formation of $OH^\bullet$ and $O_2^{-\bullet}$ and increasing the defragmentation of the dye's organic structure, which leads to a decrease in the TOC. Once an acidity equilibrium is reached between the solution/TiO_2, the surrounding pH shifts to become more alkaline, and the protons existing in the solution

tend to enter into a reaction with titania, which increases its acidity. The positively charged sites on the support increase, leading to a repulsion phenomenon between functional groups and positively charged dye molecules. Although this repulsion limits the adsorption process, the free radicals present in the solution generated by the ionization of H_2O molecules contribute to the degradation of the dye until total mineralization. Similar findings were reported by Kyung et al. [38] when investigating the removal of dyes using titanium dioxide in the presence of metals.

2.3. Regeneration Experiment

In order to investigate the possibility of using the catalyst in multiple experimental conditions for multiple times, the regeneration of the catalyst was followed for five cycles according to the experimental conditions cited in the Section 3.2.4. The results depicted in Figure 11 show that the degradation of MB in presence of zinc remained significantly high, even after using the catalyst for five consecutive cycles. The slight decrease in terms of degradation efficiency, estimated as 7.75% by the fifth cycle, could be attributed to the cumulated amount of MB by-products that remained adsorbed at the catalyst and occupied the functional groups, thus preventing the adsorption and the degradation of additional dye molecules [40]. It is also possible that this decrease is attributed to the decrease in the catalyst dose, since the recovered TiO_2 mass slightly decreased after each experiment.
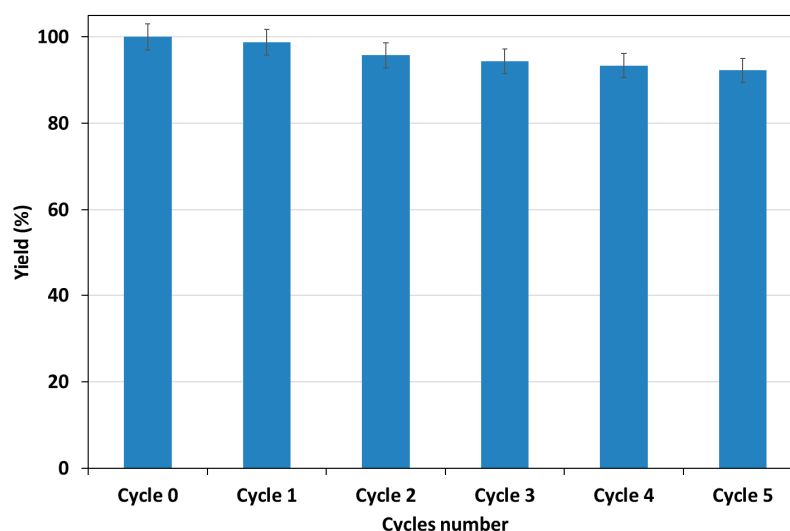

Figure 11. Discoloration percentage of methylene blue after five consecutive uses of the same photocatalyst ($C_{0, MB}$ = 60 mg/L, $C_{0, Zn^{2+}}$ = 60 mg/L pH neutral, D_{TiO_2} = 1 g/L; temperature = 20 $\pm$ 2 °C).

3. Materials and Methods

3.1. Chemicals

Methylene blue ($C_{16}H_{18}ClN_3S$, MW = 319.852 g/mol, purity = 98%), acquired from Sigma-Aldrich (Saint Louis, MO, USA), was used during the adsorption/photocatalysis experiments. A stock of 1 g/L, prepared with ultra-pure water, was used throughout the study, and desired initial dye concentrations were prepared by diluting the appropriate volume of the prepared solution. Titanium Dioxide (TiO_2) (P25 Anatase, Purity > 99%, specific surface area 350–400 m^2/g, crystallites mean size = 5–10 nm) was acquired from Millennium Inorganic Chemicals (Thann, France). Zinc nitrate (zinc nitrate hexahydrate, $Zn(NO_3)_2 \cdot 6H_2O$, MW = 297.49 g/mol purity $\geq$ 98%), acquired from Sigma-Aldrich (Saint Louis, MO, USA), was used in the batch combined pollution experiment. A Stock Zn^{2+} solution of 1 g/L was also prepared, and further dilution was performed to obtain the desired concentrations of zinc. Nitric acid (HNO3, MW = 63.01 g/mol, purity 60%) and Sodium Hydroxide (NaOH, MW = 40.00 g/mol) were purchased form Carlo Erba Reagents (Peypin, France) and were used for modification of solutions' pH.

3.2. Procedure and Analysis

3.2.1. Experimental Set-Up

Photocatalysis experiments were performed using a cylindrical batch reactor, with 76 mm as the upper diameter and 400 mm of working height, availing 1.5 L of the studied solution. A UV lamp could be inserted inside the reactor from above using a central glass tube (Ø = 50 mm), allowing 85% of the UV radiation to go through at an intensity of 40 W/m^2. The reactor contains two septa for O_2 injection and sample extractions (Figure S1). The photon excitation was provided by a Philips PL-S 9W/10/4P UV lamp (Amsterdam, Netherlands), delivering a spectral emission range between 350 and 390 nm. All experiments were performed by introducing 750 mL of aqueous solution in the reactor at the desired pollutants and photocatalyst concentrations. The system was kept at room temperature (20 ± 2 °C) to avoid solution overheating. In order to maintain a homogeneous partition of the dye and the catalyzer, the solution was continuously stirred at 200 rpm. The MB concentration at equilibrium was evaluated by measuring the absorbance decrease at 664 nm using UV-visible, spectrophotometer apparatus provided by Thermo Fischer Scientific (Waltham, MA, USA). Small volumes were extracted from the reactor to carry out the appropriate analysis and did not exceed 5% of the total aqueous solution volume present in the reactor. Appropriate dilutions were performed to fit the calibration curve.

SEM/EDX analysis provided an enlarged view of the TiO_2 catalyst sample (Figure S2). SEM/EDX analysis revealed the different elements of the catalyst, such as titanium, carbon, and oxygen, which were also previously found in cotton TiO_2. Moreover, Figure S2 shows a uniform Ti distribution in cellulosic fibers.

3.2.2. Single Type Pollution: Methylene Blue Degradation

To optimize the photocatalyst dose in the batch mode process, a preliminary experiment was performed by varying the quantity of TiO_2 set in suspension with MB aqueous solution. For this purpose, three doses of TiO_2 (e.g., 0.5, 1, and 1.5 g/L), were mixed with 60 mg/L of MB solution at pH = 6.0 and 20 ± 2 °C and continuously stirred until equilibrium was reached.

Methylene blue degradation was investigated under various experimental conditions. The initial dye concentration effect on degradation efficiency was followed for a range of concentrations between 30 and 120 mg/L. The effect of pH was carried out by varying the initial solution pH (4, 5, 6 and 8) with diluted NaOH and HNO_3 solutions (0.1 M). The effect of ionic competition on dye degradation was also followed in the presence of 0.001, 0.01 and 0.1 M NaCl aqueous concentrations.

3.2.3. Combined Pollution: Methylene Blue Degradation in Presence of Zinc II Ions

To simulate a real industrial wastewater, the photodegradation of MB in case of a simultaneous organic and inorganic pollution was studied. Initially, a fixed MB concentration of 60 mg/L was stirred in batch mode in the presence of Zn^{2+} ions at initial concentrations of 30, 60, 90 and 120 mg/L at fixed a pH, temperature, and TiO_2 dose of 6.0, 20 ± 2 °C, and 1 g/L, respectively. A matrix of experiments, presented in Table 3, was then elaborated for different initial dye and zinc concentrations to reach a better understanding of the possible interactions that might occur in the system during the simultaneous variation of organic and inorganic pollution. Zinc concentration in the solution was determined using a Shimadzu AA-6200 atomic absorption spectrometry unit (Kyoto, Japan) at an absorption wavelength of 213.9 nm.

3.2.4. Regeneration experiment

The reusability of titanium dioxide was observed at neutral pH for a contact time of 60 min for five consecutive cycles under the following conditions: $C_{0,\,MB}$ = 60 mg/L, $C_{0,\,Zn^{2+}}$ = 60 mg/L and D_{TiO_2} = 1 g/L. At the end of each experiment, the remaining solution was filtered using a vacuum pump, and the TiO_2 powder was recovered using 0.22 μm

Durapore $^{\circledR}$ PVDF membrane filters. The catalyst was the dried at 70 °C for 24 h and reused for the next experiment. The MB removal yield (Y, %) was chosen as the efficiency response.

3.2.5. Kinetic and Isotherm Adsorption Studies

At equilibrium, the amount of adsorbed MB (q_e (mg/g)) and the corresponding removal yield (Y_e (%)) were calculated using the following equations:

$$q_e = \frac{C_0 - C_e}{M} \times V \tag{6}$$

$$Y_e(\%) = \frac{C_0 - C_e}{C_0} \times 100 \tag{7}$$

where C_0 and C_e are the dye concentrations initially and at equilibrium, respectively (mg/L); M is the used photocatalyst mass (g); and V is the MB solution volume (L).

For MB adsorption modeling in the absence of UV radiation, several models have been used to describe the dynamic and equilibrium adsorption experimental data. In the present study, the most common kinetic and equilibrium models, namely, the pseudo-first-order, the pseudo-second-order, and the Freundlich and Langmuir models, respectively [10], were used. The goodness of fit of the theoretical kinetic and isotherm data with the experimental ones was judged by calculating the corresponding average percentage errors (APE) [3]:

$$APE_{kinetic}(\%) = \frac{\sum \left[(q_{t,exp} - q_{t,calc}) / q_{t,exp} \right]}{N} \times 100 \tag{8}$$

$$APE_{isotherm}(\%) = \frac{\sum \left[(q_{e,exp} - q_{e,calc}) / q_{e,exp} \right]}{N} \times 100 \tag{9}$$

where $q_{t,exp}$ and $q_{t,calc}$ (mg/g) are the experimental and the calculated adsorbed amounts at a given time, "t", respectively; $q_{e,exp}$ and $q_{e,calc}$ (mg/g) are the experimental and the calculated adsorbed amounts at equilibrium, respectively; and N is the number of the experimental runs. This section will be divided into subheadings. It should provide a concise and precise description of the experimental results, their interpretation, as well as the experimental conclusions that can be drawn.

4. Conclusions

Methylene blue degradation in aqueous solutions through the photocatalysis process in presence of Titanium dioxide (TiO_2) in suspension, at different physicochemical experimental conditions and in the presence of salt and heavy metal ions, was investigated. MB adsorption was studied in the absence of UV irradiation, and the kinetic data were well described by the pseudo-second-order kinetics model, suggesting a chemisorption process. The related equilibrium data were well suited by the Langmuir model with a maximum adsorption capacity of about 34.0 mg/L. Additionally, MB photodegradation in the presence of UV radiation was also studied under different experimental conditions. Results proved that dye photodegradation rate decreased with increasing initial organic dye concentrations due to the possible screen effect resulting from MB accumulation on the semi-conductor surface, thereby abating the electron transfer process. Moreover, dye photodegradation increased with pH increase due to the rise in fixing sites on the TiO_2 surface, allowing better retention of dye, and hence, greater organic molecule dismantling. The variation of catalyst dose and ion competition effect showed particular behavior since the MB photodegradation rate increased until reaching a plateau and then decreased gradually. These modifications are intimately related to solution pH variation during the photodegradation process. Multicomponent pollution was also investigated by adding different heavy metal ion concentrations, namely zinc (Zn^{2+}), and results manifested an enhancement of the MB photodegradation rate at low inorganic concentrations, with high Kc and low k parameters, reaching an optimum at the concentration of $[Zn^{2+}]$ = 60 mg/L. Improvement

of the photodegradation process may be explained by the possible interference of metal ions in the generation of $^{\bullet}$OH free radicals, favoring the elimination of MB.

References

1. Yagub, M.T.; Sen, T.K.; Afroze, S.; Ang, H.M. Dye and its removal from aqueous solution by adsorption: A review. *Adv. Colloid Interface Sci.* **2014**, *209*, 172–184. [CrossRef] [PubMed]
2. Verma, A.K.; Dash, R.R.; Bhunia, P. A review on chemical coagulation/flocculation technologies for removal of colour from textile wastewaters. *J. Environ. Manag.* **2012**, *93*, 154–168. [CrossRef]
3. Azzaz, A.A.; Jellali, S.; Assadi, A.A.; Bousselmi, L. Chemical treatment of orange tree sawdust for a cationic dye enhancement removal from aqueous solutions: Kinetic, equilibrium and thermodynamic studies. *Desalination Water Treat.* **2015**, *3994*, 1–13. [CrossRef]
4. Azzaz, A.A.; Jellali, S.; Akrout, H.; Assadi, A.A.; Bousselmi, L. Dynamic investigations on cationic dye desorption from chemically modified lignocellulosic material using a low-cost eluent: Dye recovery and anodic oxidation efficiencies of the desorbed solutions. *J. Clean. Prod.* **2018**, *201*, 28–38. [CrossRef]
5. Kim, J.R.; Kan, E. Heterogeneous photo-Fenton oxidation of methylene blue using CdS-carbon nanotube/TiO$_2$ under visible light. *J. Ind. Eng. Chem.* **2015**, *21*, 644–652. [CrossRef]
6. Khandare, R.V.; Govindwar, S.P. Phytoremediation of textile dyes and effluents: Current scenario and future prospects. *Biotechnol. Adv.* **2015**, *33*, 1697–1714. [CrossRef] [PubMed]
7. Al jibouri, A.K.H.; Wu, J.; Upreti, S.R. Continuous ozonation of methylene blue in water. *J. Water Process Eng.* **2015**, *8*, 142–150. [CrossRef]
8. Madhavan, J.; Kumar, P.S.S.; Anandan, S.; Grieser, F.; Ashokkumar, M. Degradation of acid red 88 by the combination of sonolysis and photocatalysis. *Sep. Purif. Technol.* **2010**, *74*, 336–341. [CrossRef]
9. Pereira, J.H.O.S.; Reis, A.C.; Queirós, D.; Nunes, O.C.; Borges, M.T.; Vilar, V.P.; Boaventura, R.A.R. Insights into solar TiO$_2$-assisted photocatalytic oxidation of two antibiotics employed in aquatic animal production, oxolinic acid and oxytetracycline. *Sci. Total Environ.* **2013**, *463–464*, 274–283. [CrossRef] [PubMed]
10. Azzaz, A.A.; Jellali, S.; Akrout, H.; Assadi, A.A.; Bousselmi, L. Optimization of a cationic dye removal by a chemically modified agriculture by-product using response surface methodology: Biomasses characterization and adsorption properties. *Environ. Sci. Pollut. Res.* **2017**, *24*, 9831–9846. [CrossRef]
11. Zeghioud, H.; Khellaf, N.; Amrane, A.; Djelal, H.; Elfalleh, W.; Assadi, A.A.; Rtimi, S. Photocatalytic performance of TiO$_2$ impregnated polyester for the degradation of Reactive Green 12: Implications of the surface pretreatment and the microstructure. *J. Photochem. Photobiol. A Chem.* **2017**, *346*, 493–501. [CrossRef]
12. Costa, G.; Assadi, A.A.; Ghaida, S.G.; Bouzaza, A.; Wolbert, D. Study of butyraldehyde degradation and by-products formation by using a surface plasma discharge in pilot scale: Process modeling and simulation of relative humidity effect. *Chem. Eng. J.* **2017**, *307*, 785–792. [CrossRef]
13. Assadi, A.A.; Bouzaza, A.; Soutrel, I.; Petit, P.; Medimagh, K.; Wolbert, D. A study of pollution removal in exhaust gases from animal quartering centers by combining photocatalysis with surface discharge plasma: From pilot to industrial scale. *Chem. Eng. Process. Process Intensif.* **2017**, *111*, 1–6. [CrossRef]
14. Assadi, A.A.; Bouzaza, A.; Wolbert, D. Study of synergetic effect by surface discharge plasma/TiO$_2$ combination for indoor air treatment: Sequential and continuous configurations at pilot scale. *J. Photochem. Photobiol. A Chem.* **2015**, *310*, 148–154. [CrossRef]
15. Ngah, W.S.W.; Hanafiah, M.A.K.M. Removal of heavy metal ions from wastewater by chemically modified plant wastes as adsorbents: A review. *Bioresour. Technol.* **2008**, *99*, 3935–3948. [CrossRef]
16. Moussa, H.; Girot, E.; Mozet, K.; Alem, H.; Medjahdi, G.; Schneider, R. ZnO rods/reduced graphene oxide composites prepared via a solvothermal reaction for efficient sunlight-driven photocatalysis. *Appl. Catal. B Environ.* **2016**, *185*, 11–21. [CrossRef]
17. Aghdasinia, H.; Bagheri, R.; Vahid, B.; Khataee, A. Central composite design optimization of pilot plant fluidized-bed heterogeneous Fenton process for degradation of an azo dye. *Environ. Technol. (United Kingdom)* **2016**, *37*, 2703–2712. [CrossRef]

18. Sun, H.; Liu, S.; Liu, S.; Wang, S. A comparative study of reduced graphene oxide modified TiO_2, ZnO and Ta_2O_5 in visible light photocatalytic/photochemical oxidation of methylene blue. *Appl. Catal. B Environ.* **2014**, *146*, 162–168. [CrossRef]

19. Azzaz, A.A.; Assadi, A.A.; Jellali, S.; Bouzaza, A.; Wolbert, D.; Rtimi, S.; Bousselmi, L. Discoloration of simulated textile effluent in continuous photoreactor using immobilized titanium dioxide: Effect of zinc and sodium chloride. *J. Photochem. Photobiol. A Chem.* **2018**, *358*, 111–120. [CrossRef]

20. Azzaz, A.A.; Jellali, S.; Jeguirim, M.; Bousselmi, L.; Bengharez, Z.; Akrout, H. Optimization of a cationic dye desorption from a loaded-lignocellulosic biomass: Factorial design experiments and investigation of mechanisms. *Comptes Rendus. Chim.* **2021**, *24*, 1–14. [CrossRef]

21. Wang, N.; Chen, J.; Wang, J.; Feng, J.; Yan, W. Removal of methylene blue by Polyaniline/TiO_2 hydrate: Adsorption kinetic, isotherm and mechanism studies. *Powder Technol.* **2019**, *347*, 93–102. [CrossRef]

22. Jafari, S.; Azizian, S.; Jaleh, B. Adsorption kinetics of methyl violet onto TiO_2 nanoparticles with different phases, Colloids Surfaces A Physicochem. *Eng. Asp.* **2011**, *384*, 618–623. [CrossRef]

23. Kanakaraju, D.; Motti, C.A.; Glass, B.D.; Oelgemöller, M. TiO_2 photocatalysis of naproxen: Effect of the water matrix, anions and diclofenac on degradation rates. *Chemosphere* **2015**, *139*, 579–588. [CrossRef]

24. Lachheb, H.; Puzenat, E.; Houas, A.; Ksibi, M.; Elaloui, E.; Guillard, C.; Herrmann, J.M. Photocatalytic degradation of various types of dyes (Alizarin S, Crocein Orange G, Methyl Red, Congo Red, Methylene Blue) in water by UV-irradiated titania. *Appl. Catal. B Environ.* **2002**, *39*, 75–90. [CrossRef]

25. Kanakaraju, D.; Glass, B.D.; Oelgemöller, M. Titanium dioxide photocatalysis for pharmaceutical wastewater treatment. *Environ. Chem. Lett.* **2014**, *12*, 27–47. [CrossRef]

26. Devi, L.G.; Murthy, B.N.; Kumar, S.G. Photocatalytic activity of TiO_2 doped with Zn^{2+} and V^{5+} transition metal ions: Influence of crystallite size and dopant electronic configuration on photocatalytic activity. *Mater. Sci. Eng. B Solid-State Mater. Adv. Technol.* **2010**, *166*, 1–6. [CrossRef]

27. Laysandra, L.; Sari, M.W.M.K.; Soetaredjo, F.E.; Foe, K.; Putro, J.N.; Kurniawan, A.; Ju, Y.H.; Ismadji, S. Adsorption and photocatalytic performance of bentonite-titanium dioxide composites for methylene blue and rhodamine B decoloration. *Heliyon* **2017**, *3*, e00488. [CrossRef]

28. Wang, H.; Zhou, P.; Guo, R.; Wang, Y.; Zhan, H.; Yuan, Y. Synthesis of rectorite/Fe3O4/ZnO composites and their application for the removal of methylene blue dye. *Catalysts* **2018**, *8*, 107. [CrossRef]

29. Wang, Y.; Jiang, L. Roles of Graphene Oxide in Hydrothermal Carbonization and Microwave Irradiation of Distiller's Dried Grains with Solubles to Produce Supercapacitor Electrodes. *ACS Sustain. Chem. Eng.* **2017**, *5*, 5588–5597. [CrossRef]

30. Szostak, K.; Banach, M. Sorption and photocatalytic degradation of methylene blue on bentonite-ZnO-CuO nanocomposite. *J. Mol. Liq.* **2019**, *286*, 110859. [CrossRef]

31. Wang, S.; Zhou, Y.; Han, S.; Wang, N.; Yin, W.; Yin, X.; Gao, B.; Wang, X.; Wang, J. Carboxymethyl cellulose stabilized ZnO/biochar nanocomposites: Enhanced adsorption and inhibited photocatalytic degradation of methylene blue. *Chemosphere* **2018**, *197*, 20–25. [CrossRef]

32. Fatimah, I.; Wang, S.; Wulandari, D. ZnO/montmorillonite for photocatalytic and photochemical degradation of methylene blue. *Appl. Clay Sci.* **2011**, *53*, 553–560. [CrossRef]

33. Baaloudj, O.; Nasrallah, N.; Kebir, M.; Guedioura, B.; Amrane, A.; Nguyen-Tri, P.; Nanda, S.; Assadi, A.A. Artificial neural network modeling of cefixime photodegradation by synthesized $CoBi_2O_4$ nanoparticles. *Environ. Sci. Pollut. Res.* **2021**, *28*, 15436–15452. [CrossRef] [PubMed]

34. Karoui, S.; Arfi, R.B.; Ghorbal, A.; Amrane, A.; Assadi, A.A. Innovative sequential combination of fixed bed adsorption/desorption and photocatalysis cost-effective process to remove antibiotics in solution. *Prog. Org. Coat.* **2021**, *151*, 106014. [CrossRef]

35. Rabahi, A.; Assadi, A.A.; Nasrallah, N.; Bouzaza, A.; Maachi, R.; Wolbert, D. Photocatalytic treatment of petroleum industry wastewater using recirculating annular reactor: Comparison of experimental and modeling. *Environ. Sci. Pollut. Res.* **2019**, *26*, 19035–19046. [CrossRef] [PubMed]

36. Zeghioud, H.; Assadi, A.A.; Khellaf, N.; Djelal, H.; Amrane, A.; Rtimi, S. Photocatalytic performance of $CuxO/TiO_2$ deposited by HiPIMS on polyester under visible light LEDs: Oxidants, ions effect, and reactive oxygen species investigation. *Materials* **2019**, *12*, 412. [CrossRef] [PubMed]

37. Kamagate, M.; Assadi, A.A.; Kone, T.; Giraudet, S.; Coulibaly, L.; Hanna, K. Use of laterite as a sustainable catalyst for removal of fluoroquinolone antibiotics from contaminated water. *Chemosphere* **2018**, *195*, 847–853. [CrossRef] [PubMed]

38. Kyung, H.; Lee, J.; Choi, W. Simultaneous and synergistic conversion of dyes and heavy metal ions in aqueous TiO_2 suspensions under visible-light illumination. *Environ. Sci. Technol.* **2005**, *39*, 2376–2382. [CrossRef]

39. Almansba, A.; Kane, A.; Nasrallah, N.; Lamaa, L.; Peruchon, L.; Brochier, C.; Béchohra, I.; Amrane, A.; Assadi, A.A. Innovative photocatalytic luminous textiles optimized towards water treatment: Performance evaluation of photoreactors. *Chem. Eng. J.* **2021**, *416*, 129195. [CrossRef]

40. Azzaz, A.A.; Jellali, S.; Bengharez, Z.; Bousselmi, L.; Akrout, H. Investigations on a dye desorption from modified biomass by using a low-cost eluent: Hysteresis and mechanisms exploration. *Int. J. Environ. Sci. Technol.* **2019**, *16*, 7393–7408. [CrossRef]